Journal of Applied Electrochemistry **30**: 675–683, 2000.

Electrochemical behaviour of aluminium in the presence of EDTA-containing chloride solutions

G.M. TREACY*, A.L. RUDD and C.B. BRESLIN
Department of Chemistry, National University of Ireland Maynooth, Maynooth, Co. Kildare, Ireland
*(*Present address: IPTME, Loughborough University, Loughborough, Leicestershire LE11 3TU, Great Britain)*

Received 2 July 1999; accepted in revised form 2 November 1999

Key words: aluminium, dissolution, EDTA, pitting

Abstract

The electrochemical behaviour of pure aluminium in an EDTA-containing chloride solution was investigated using potentiodynamic and potentiostatic electrochemical techniques and electrochemical impedance spectroscopy. A pronounced EDTA-induced anodic dissolution was observed in alkaline solutions, but the presence of EDTA in solution had little activating effect on the passivation properties at pH values close to 4.0. This was attributed to the relative stability of the $Al(EDTA)^-$ complex formed at the different pH values. This EDTA-induced activation had no deleterious effect on pitting attack, in fact, higher breakdown potentials were observed in the presence of EDTA. This was attributed to the buffering action of EDTA, which inhibited the attainment of a critical pit solution composition. But, in the presence of molybdate, EDTA had no observable effect on pitting attack. The impedance spectra recorded in the presence of EDTA showed evidence for the adsorption of EDTA species during the dissolution process, which in turn, form a large capacitive network, with capacitance values of the order of 3 mF cm^{-2} in the low frequency region.

1. Introduction

Ethylenediaminetetraacetic acid (EDTA), is a well-known chelating agent [1]. EDTA-containing solutions are used as cleaning agents for the removal of iron oxide and other scales in many heat-exchange systems. In some cases, the EDTA treatment gives rise to increased corrosion or dissolution of the metal, while in other situations, EDTA or EDTA complexes can have a beneficial effect in reducing the corrosion rate of some metals.

For example, Palmer and Boden [2], in studying the corrosion of steel in EDTA-containing solutions, found that EDTA acts as a cathodic stimulant inducing high rates of corrosion even in the absence of oxygen. They found evidence for the reduction of the EDTA–carboxylic acid groups to aldehyde and hydroxy groups, indicating the reduction of EDTA at the electrode surface. Nahle [3] found that EDTA increased the rate of dissolution of tin through the formation of a Sn(II)-EDTA complex. Healy and Ducheyne [4] reported the enhanced dissolution of titanium in a simulated interstitial electrolyte to which EDTA was added. On the other hand, Alhajji and Reda [5] found that EDTA had a beneficial effect in reducing the rate of corrosion of several copper-nickel alloys in sulfide-polluted seawater. Capobianco et al. [6] found that a complex of EDTA, Fe(II)-EDTA hydroxylamine sulfate, acted as a corrosion inhibitor for type SS316L steel in a crystallization plant.

Although the presence of EDTA in an environment has considerable effects on the corrosion susceptibility of many materials, these systems have received little attention. In this communication, results, on the influence of EDTA on the electrochemical behaviour of pure aluminium, are reported.

2. Experimental details

Polycrystalline aluminium electrodes, (99.9999% purity) were provided in rod form. These rods were abraded, with suspensions of diamond paste to a mirror finish. After cleaning with ethanol and distilled water, the electrodes were mounted in resin so as to expose a circular face, 0.8 cm^2 in area, to the test solution.

Test solutions consisted of 0.005, 0.01 and 0.025 mol dm^{-3} EDTA (disodium salt), with and without the addition of 0.1 mol dm^{-3} NaCl. These were prepared using AnalaR grade reagents and deionised water. The pH of the solutions was adjusted to the desired pH using H_2SO_4 and NaOH. The electrochemical cell consisted of a pyrex glass cell, a saturated calomel reference electrode and graphite auxiliary electrodes.

Electrochemical measurements were performed with a PAR model 263 potentiostat controlled by the model

352 corrosion-measurement/software package. Potentiodynamic scans were carried out using a scan rate of 1.0 mV s^{-1}. The scan was initiated at −1600 mV vs SCE and terminated at the pitting potential. The electrodes were first polarized at −1600 mV vs SCE for 5 min prior to polarization in the anodic direction. AC impedance measurements were recorded using a Solartron 1250 frequency response analyser and an EI 1287 electrochemical interface. The spectra were recorded at an applied potential following various periods of polarization. An excitation voltage of 10 mV was used. All impedance data were fit to appropriate equivalent circuits using a complex nonlinear least squares fitting routine, using both the real and imaginary components of the data.

3. Results

Representative anodic polarization plots, recorded for aluminium in 0.1 mol dm^{-3} NaCl solution and in 0.1 mol dm^{-3} NaCl solution to which 0.01, 0.025 and 0.005 mol dm^{-3} EDTA was added are presented in Figure 1(a) and (b). The plots presented in Figure 1(a) were recorded at pH 7.0 and the data in Figure 1(b) were recorded at pH 9.0. It can be seen from these plots that the presence of EDTA in the chloride-containing solution leads to an increase in the passive current density, an increase in the corrosion current, and a negative displacement in the corrosion potential. These effects are consistent with an increase in the anodic dissolution rate of aluminium. It is evident also that the greatest degree of activation occurs in the more alkaline pH 9.0 solution, where the anodic current in the potential region from −1.2 to −0.80 V is approximately two orders of magnitude higher in the presence of EDTA. The presence of EDTA in solution has little effect on the pitting potential of aluminium in the pH 7.0 solution, but slightly more noble breakdown potentials are recorded in the pH 9.0 EDTA-containing solution. This is most likely associated with the buffering action of the EDTA complex, which inhibits the local acidification process which occurs on the initiation and propagation of pits [7, 8] and thus leads to apparently higher breakdown potentials. A similar degree of activation was observed in the absence of chloride. The passive current density recorded on polarising pure aluminium in a 0.01 mol dm^{-3} EDTA solution in the absence of chloride was of the order of 60 μA cm^{-2}, slightly lower than that recorded in the presence of chloride. However, with increasing acidity of the solution, pH values less than 4.0, this activation effect was removed, and indeed in some cases slightly lower passive currents were observed in the acidic EDTA solution than in the acidic chloride solution [9].

Current–time transients recorded at −800 mV vs SCE for aluminium in the presence and absence of EDTA in the pH 9.0 and 7.0 solutions are shown in Figure 2(a) and (b), respectively. Here, it can be seen that the active

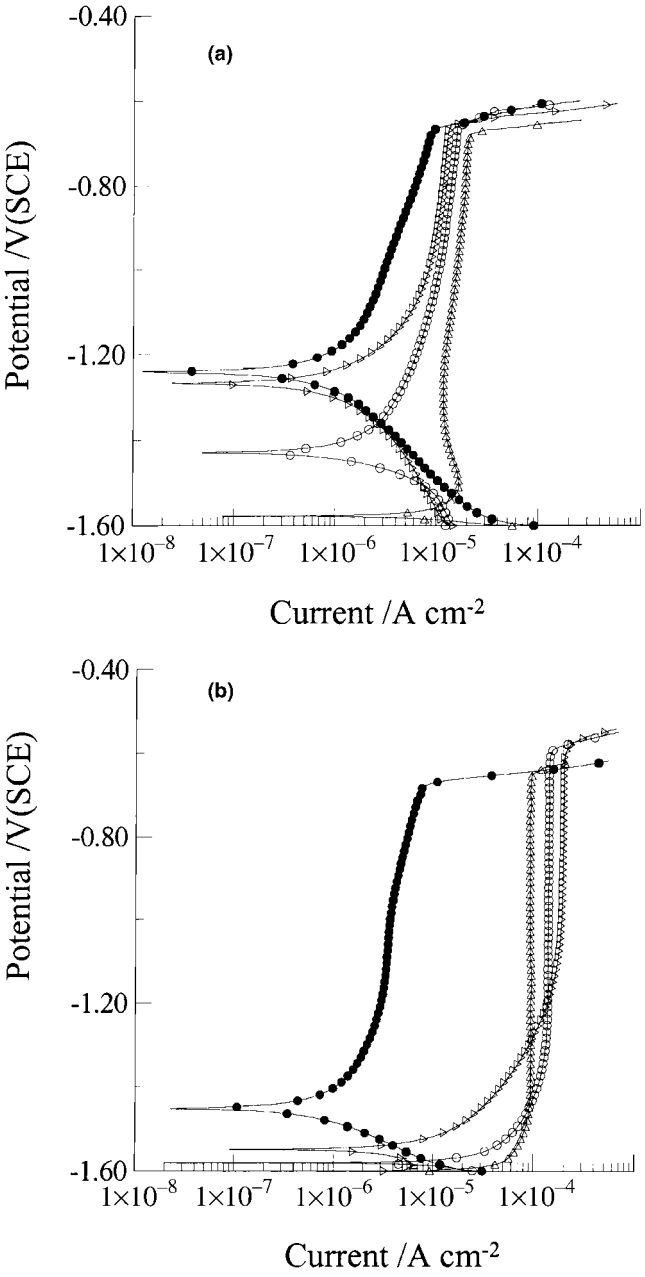

Fig. 1. Anodic polarization plots recorded for aluminium in 0.1 mol dm^{-3} NaCl in the (●) absence and presence of (▷) 0.005, (○) 0.01 and (△) 0.025 mol dm^{-3} EDTA at pH values of (a) 7.0 and (b) 9.0.

conditions induced by the EDTA species are maintained over long time periods. The anodic current decays in a continuous manner in the absence of EDTA, as the passive film is formed, however in the presence of EDTA, the current reaches a steady-state condition within 200 s. Although there is little difference in the passive currents recorded in the pH 7.0 and 9.0 solutions in the absence of EDTA, the anodic current is approximately an order of magnitude higher at pH 9.0 in the presence of EDTA.

To gain information on the thickness of the passive layers formed in the presence and absence of EDTA, capacitance measurements were performed on alumin-

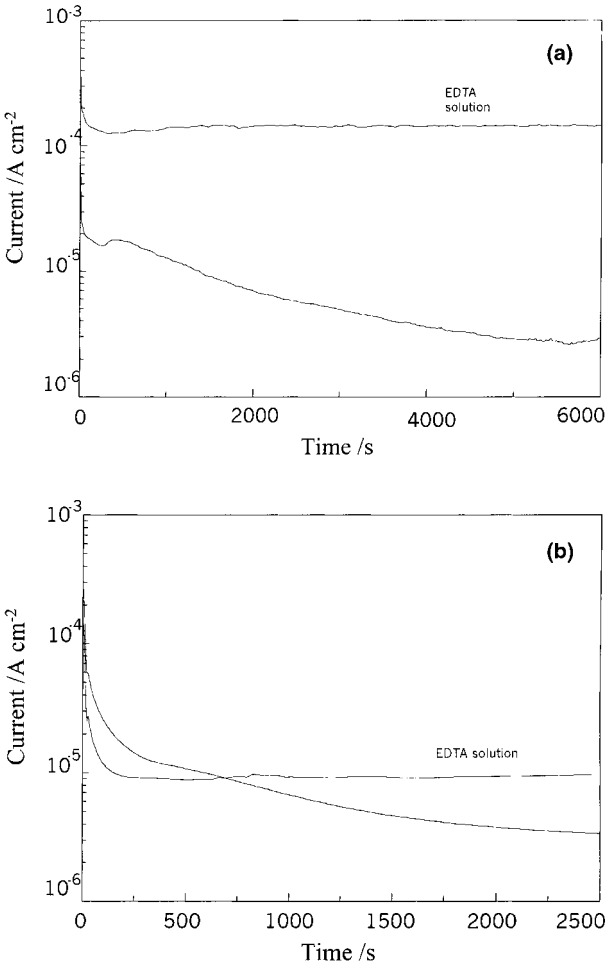

Fig. 2. Current–time transients recorded at −800 mV for aluminium polarized in 0.1 mol dm^{-3} NaCl containing 0.01 mol dm^{-3} EDTA at pH 9.0 (a) and pH 7.0 (b).

ium polarized in these solutions. These data were obtained by polarizing aluminium at a scan rate of 0.2 mV s^{-1} from −1600 mV up to the pitting potential. A 10 mV perturbation signal (1 or 5 kHz) was superimposed on this positive potential sweep and the imaginary impedance and capacitance measured as a function of the applied potential. Assuming that the passive layer behaves as a dielectric, then the measured capacitance is proportional to the thickness of the passive layer, Equation 1:

$$d = \frac{\varepsilon\varepsilon_0 A}{C} \tag{1}$$

Here d is the thickness of the passive layer, ε_0 is the vacuum permitivity and ε is the dielectric constant of the passive layer.

In Figure 3 the capacitance measured as a function of applied potential for aluminium polarised in the pH 7.0 and 9.0 solutions in the presence and absence of EDTA are shown. Data are shown for both the 1 and 5 kHz measurements in the case of the pH 7.0 solution. Although there is evidence of a frequency dispersion in these data, it is clear that the presence of EDTA has

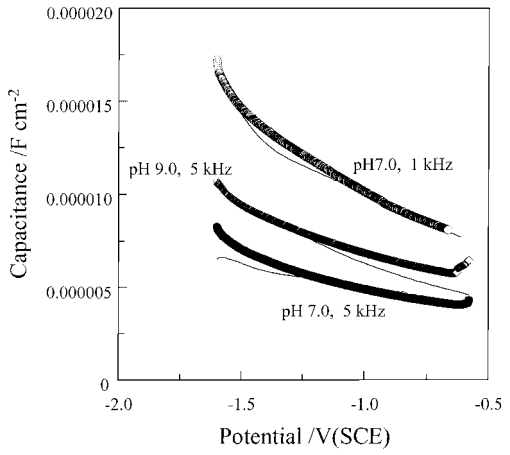

Fig. 3. Capacitance–voltage relationship for aluminium, measured at 1 kHz and polarised in 0.1 mol dm^{-3} NaCl, pH 7.0 in the absence of EDTA (—), in the presence of 0.01 mol dm^{-3} EDTA (○); measured at 5 kHz, in the absence of EDTA (—), in the presence of 0.01 mol dm^{-3} EDTA (●); measured at 5 kHz and in pH 9.0 solution, in the absence of EDTA (—), and in the presence of 0.01 mol dm^{-3} EDTA (◇).

little effect on the measured capacitance and thus, the thickness of the passive layer.

The open-circuit potentials adopted by aluminium in the pH 7.0 and 9.0 solutions in the presence and absence of EDTA are shown in Figure 4. The open-circuit potentials in the absence of EDTA lie in the region from −750 to −1000 mV vs SCE as expected [10, 11]. However, when EDTA is added to the solution, the open-circuit potential is displaced by up to 700 mV. These active potentials are maintained indefinitely. It is also evident here, in agreement with the anodic polarization data that the greatest displacement in the open-circuit potential occurs in the more alkaline solution. Again, these negative open-circuit potentials are consistent with the increased anodic dissolution induced by EDTA.

In Figure 5(a) and (b) impedance spectra are shown for aluminium polarised at −800 mV vs SCE in the pH 7.0 solution in the absence and presence of EDTA, respectively. These data are shown as a function of the polarization period for periods of 60, 260, 460, 660 and

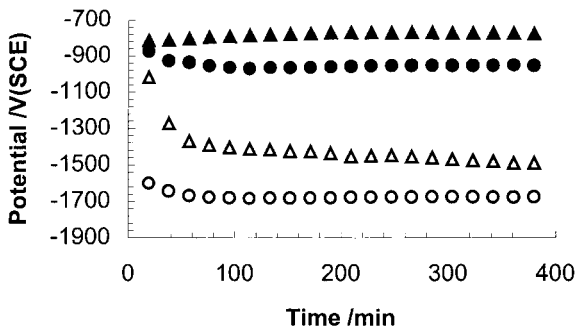

Fig. 4. Open-circuit potential–time plots recorded for aluminium in 0.1 mol dm^{-3} NaCl solution at pH 7.0 (▲), and pH 9.0 (●), and in 0.1 mol dm^{-3} NaCl and 0.01 mol dm^{-3} EDTA at pH 7.0 (△) and 9.0 (○).

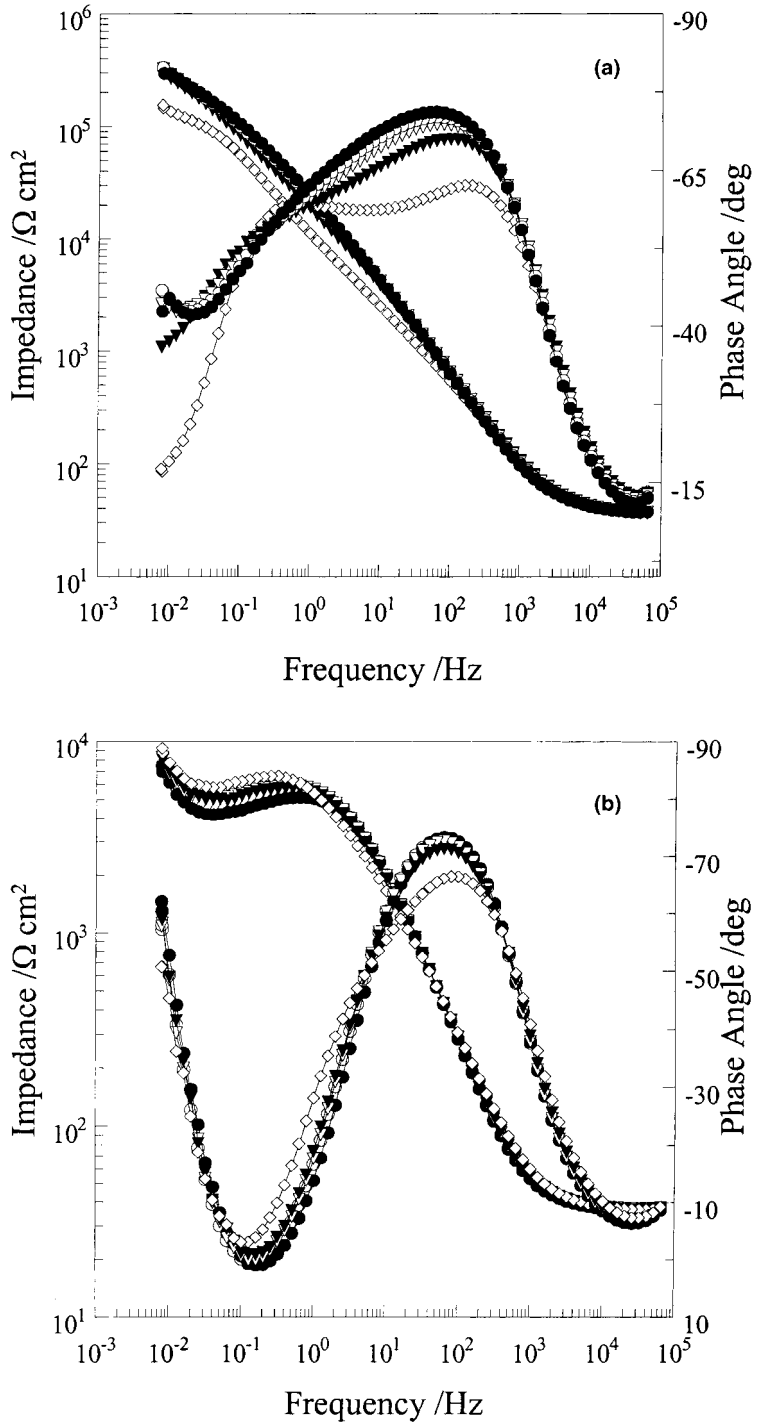

Fig. 5. Complex impedance spectra recorded for aluminium at −800 mV vs SCE in (top) 0.1 mol dm^{-3} NaCl, pH 7.0 solution and (bottom) 0.1 mol dm^{-3} NaCl containing 0.01 mol dm^{-3} EDTA, pH 7.0 solution; both at time intervals of 60 min (◇), 260 min (▲), 460 min (△), 660 min (○) and 860 min (●).

860 min. The data recorded in the absence of EDTA are characteristic of a two-time constant system, with a diffusion-controlled process being clearly evident at the lower frequencies. The impedance spectra show a gradual evolution with time, but after the first 100 min of polarization there is little further change in the spectra. The impedance spectra are very different in the presence of EDTA, Figure 5(b). At least three time constants can be observed. A capacitive time constant at high frequencies, an inductive time constant at medium frequencies and a further capacitive element at low frequencies. Again, the impedance spectra remain essentially independent of the polarization period after the elapse of the first 100 min.

A similar set of data recorded, with the same time intervals, in the pH 9.0 solution is shown in Figure 6(a) and (b). Again, the data recorded in the absence of EDTA show evidence of two time constants, a high to

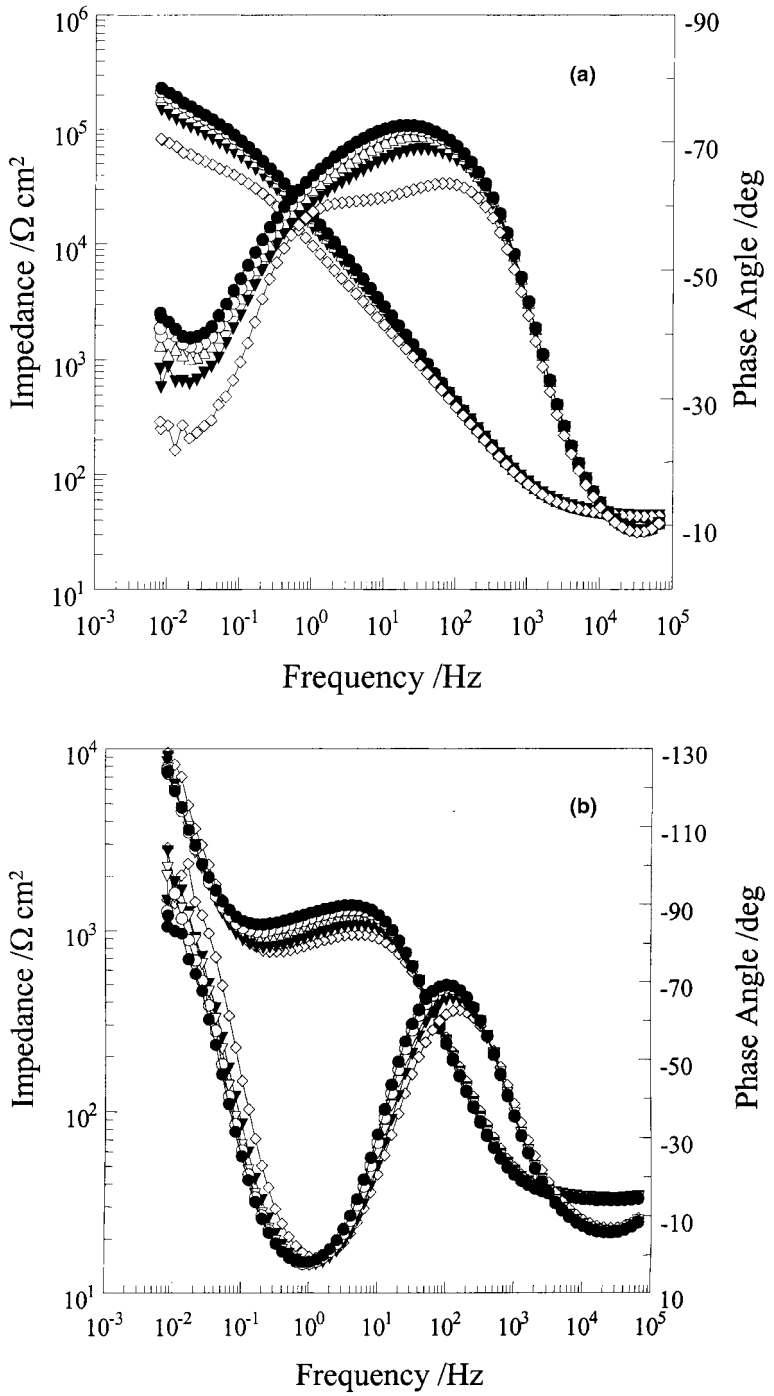

Fig. 6. Complex impedance spectra recorded for aluminium at −800 mV vs SCE in (top) 0.1 mol dm^{-3} NaCl, pH 9.0 solution and (bottom) 0.1 mol dm^{-3} NaCl containing 0.01 mol dm^{-3} EDTA, pH 9.0 solution; both at time intervals of 60 min (◇), 260 min (▲), 460 min (△), 660 min (○) and 860 min (●).

medium frequency capacitive term and a second low frequency diffusion term. After the elapse of the first 100 min the data exhibit only slight change with polarization time. The data measured in the presence of EDTA, Figure 6(b), exhibit clearly three different time constants; a high frequency capacitive region, a medium frequency inductive region and a low-frequency capacitive region where the impedance increases sharply with decreasing frequency.

These impedance data were fit to two separate circuits. The data measured in the absence of EDTA were fit to the circuit shown in Figure 7(a), which incorporates two constant phase elements, Q_1 and Q_2. The impedance of a constant-phase element, is defined as $Z_{CPE} = [Q(j\omega)^n]^{-1}$ where $-1 \leq n \leq 1$ [12]. The n value obtained in the case of Q_1 was close to 1.0 indicating that Q_1 is a true capacitor, while the n value obtained for Q_2 was 0.5 indicating that Q_2 is a Warburg diffusion term. The equivalent circuit shown in Figure 7(b) was used to fit the impedance data measured in the presence of EDTA. The n values, obtained for all three Q terms, were close to 1.0 indicating that the three constant phase

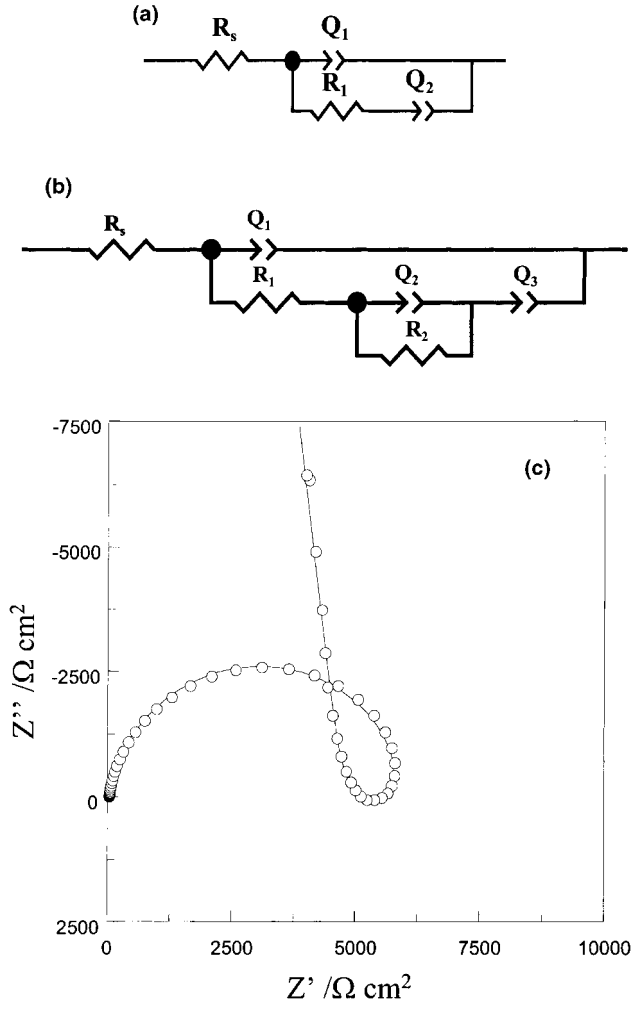

Fig. 7. (a) Equivalent circuit used to fit impedance data recorded in the absence of EDTA, (b) equivalent circuit used to fit impedance data recorded in the presence of EDTA, (c) agreement between experimental data (○), and simulated data (—) experimental data were recorded in 0.1 mol dm^{-3} NaCl containing 0.01 mol dm^{-3} EDTA, pH 7.0 solution.

elements are capacitor elements. In order to model the inductance a negative resistor, R_2, and capacitor, Q_2, was used. These negative parameters were used as opposed to using an inductor, a model based on that used by Franceschetti and Macdonald [13], Armstrong [14] and Pettersson and Pound [15] to model systems involving passivation or adsorption-type reactions. The level of agreement between the experimental data and the simulated data was excellent and can be seen in Figure 7(c), where the Nyquist plot is shown for aluminium in the presence of EDTA in the pH 7.0 solution for the experimental and simulated data.

In Figure 8, the resistance element R_1 is plotted as a function of time for aluminium polarised at −800 mV in the pH 7.0 and 9.0 solutions in the absence and presence of EDTA. R_1, which is equivalent to the polarization resistance in the case of aluminium in the absence of EDTA, is of the order of $5 \times 10^4\ \Omega\,\text{cm}^2$ in both the pH 7.0 and 9.0 solutions. However, a considerable reduction in the value of R_1 is seen on the introduction

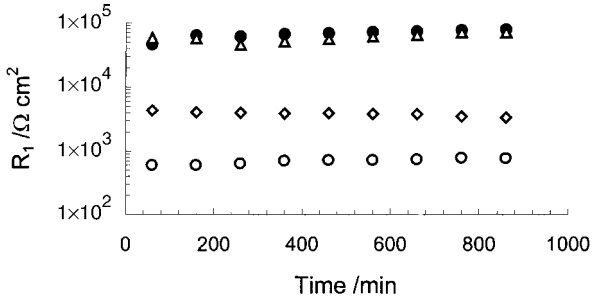

Fig. 8. R_1 plotted as a function of time for Al polarized at −800 mV vs SCE in 0.1 mol dm^{-3} NaCl, pH 9.0 solution (●); pH 7.0 solution (△); in 0.1 mol dm^{-3} NaCl containing 0.01 mol dm^{-3} EDTA, pH 9.0 solution (○); and EDTA pH 7.0 solution (◇).

of EDTA into solution. Again, the greatest change is evident in the pH 9.0 solution.

The value of R_1 plotted as a function of potential for aluminium polarized in the pH 9.0 EDTA-containing electrolyte is shown in Figure 9. The electrodes were polarized for a 2 h period at each potential and then the impedance data were recorded, after a further 100 min polarization period a second impedance measurement was performed. The values of R_1 calculated after 120 min and the 220 min period are shown on the plot. It can be seen that the magnitude of R_1 varies slightly with applied potential, reaching a maximum value at about −1100 mV vs SCE. Secondly, R_1 tends to increase slightly on further polarization at potentials between −800 and −1200 mV , but tends to decrease with further polarization at potentials more electronegative than −1200 mV.

The dependence of Q_1 and Q_3 on the applied potential can be seen in Figure 10(a) and (b) for aluminium polarized in the pH 9.0 EDTA-containing electrolyte. Q_1, which represents the double-layer capacitance, decreases on increasing the applied potential and ranges in value from 10 to 25 μF cm^{-2}. In the absence of EDTA the double layer capacitance is of the order of 6–8 μF cm^{-2}. The constant phase element, Q_3, which may be taken as a capacitance, is of the order of 1 to 3 mF cm^{-2} and increases with increasing potential.

Despite these activating effects induced by the EDTA, the presence of EDTA in solution has little effect on the pitting process. This can be seen from the data presented

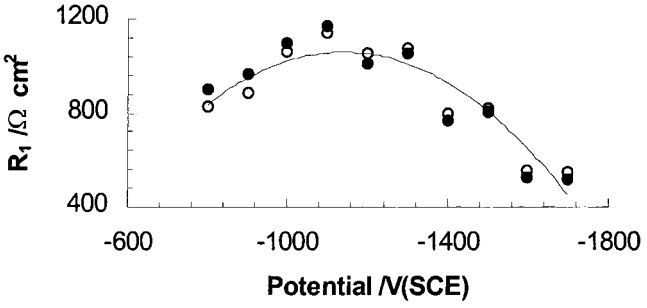

Fig. 9. R_1 plotted as a function of potential for aluminium polarized in 0.1 mol dm^{-3} NaCl containing 0.01 mol dm^{-3} EDTA, pH 9.0 solution, data recorded after 120 min (○) and after 220 min (●).

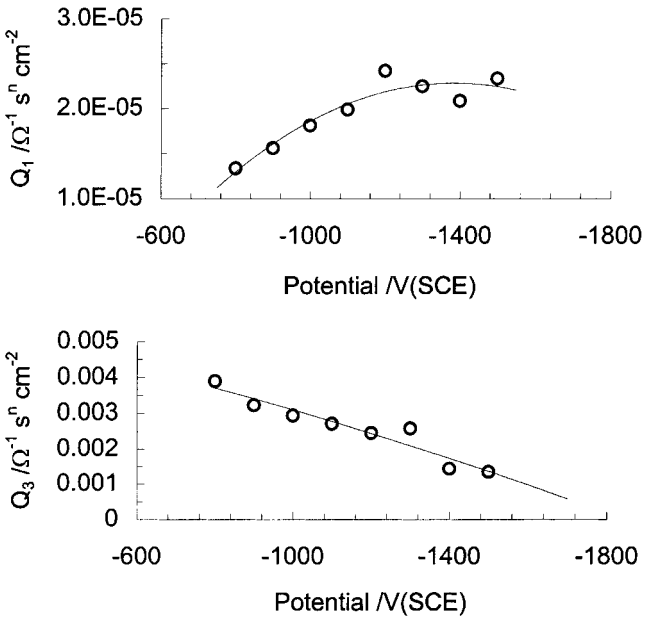

Fig. 10. (a) Q_1 and (b) Q_3 plotted as function of potential for aluminium polarized in 0.1 mol dm^{-3} NaCl solution containing 0.01 mol dm^{-3} EDTA, pH 9.0 solution.

in Figure 11 where cumulative probability plots of the pitting potentials measured in 0.1 mol dm^{-3} NaCl, in the presence and absence of EDTA and in 0.1 mol dm^{-3} NaCl containing 0.01 mol dm^{-3} Na_2MoO_4 in the presence and absence of EDTA are shown. The presence of EDTA in the 0.1 mol dm^{-3} NaCl solution has a slight inhibiting effect on the pitting process, but this is due to the buffering action of the EDTA complexing species. Of more interest is the fact that the presence of EDTA, which seems to modify considerably the activity of the passive layer, has no observable effect on the pitting potential in the presence of molybdate. Similar pitting potential distributions are seen both in the presence and absence of EDTA in the case of the molybdate-containing solutions.

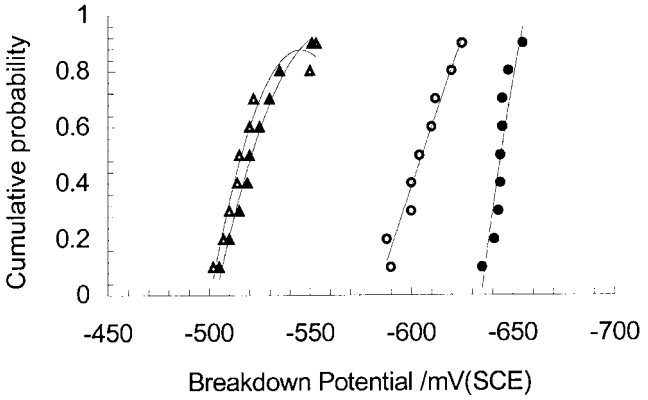

Fig. 11. Cumulative probability plots of the pitting potentials recorded in 0.1 mol dm^{-3} NaCl, pH 9.0 solution (●) in 0.1 mol dm^{-3} NaCl containing 0.01 mol dm^{-3} EDTA pH 9.0 solution (○) in 0.1 mol dm^{-3} NaCl, 0.01 mol dm^{-3} Na_2MoO_4, pH 9.0 solution (▲) and in 0.1 mol dm^{-3} NaCl, 0.01 mol dm^{-3} EDTA, 0.01 mol dm^{-3} Na_2MoO_4, pH 9.0 solution (△).

4. Discussion

It is clearly evident from the results presented that the presence of EDTA in near neutral and alkaline solution accelerates the rate of dissolution of aluminium. These effects, particularly the pH dependence, appear to be connected with the complexation chemistry of the EDTA chelant[1]. EDTA is a hexaprotic system, which can be designated as H_6Y^{2+}. Its degree of protonation depends on the pH of the solution and its ability to co-ordinate metal ions varies with the pH of the solution and the nature of the metal ions. The reaction between Al^{3+} and EDTA (H_6Y^{2+}) can be represented by the following reaction:

$$Al^{3+} + H_6Y^{2+} \rightarrow AlY^- + 6\,H^+ \tag{2}$$

where AlY^- is equivalent to $Al(EDTA)^-$. Due to the several forms of free EDTA possible it is more convenient to use the dissociation constant K' to describe the complexation reactions,

$$K' = \frac{1}{\alpha_{Y^{4-}} K_f} \tag{3}$$

where, K_f, the formation constant is equivalent to,

$$K_f = \frac{[AlY^-]}{[Al^{3+}][H_6Y^{2+}]} \tag{4}$$

and, $\alpha_{Y^{4-}}$ is defined as the fraction of EDTA present in solution in the deprotonated form and is equal to,

$$\alpha_{Y^{4-}} = \frac{[Y^{4-}]}{[H_6Y^{2+}]} \tag{5}$$

The values for $\alpha_{Y^{4-}}$ for the complexation of Al^{3+} in a 0.01 mol dm^{-3} EDTA solution are 5.4×10^{-2} at pH 9.0, 5.0×10^{-4} at pH 7.0 and 3.8×10^{-9} at pH 4.0 [1]. The values of K' are 9.3×10^{-16} at pH 9.0, 1.0×10^{-13} at pH 7.0 and 1.3×10^{-8} at pH 4.0. It can be deduced from these values that the fraction of EDTA in solution in the deprotonated form decreases considerably from pH 9.0 to 7.0 and even more significantly down to 3.8×10^{-9} at pH 4.0. It is also clear that the dissociation constant decreases as the pH increases indicating the increasing stability of the $Al(EDTA)^-$ complex with increasing pH. Thus, the increased activation, observed on polarizing Al in the pH 9.0 EDTA solution, is consistent with the low value of K'. On the other hand, the lack of any activation in the pH 4.0 solution is consistent with the low level of deprotonation of EDTA in the slightly acidic environment and the much higher K' value.

Despite this enhanced dissolution in the pH 9.0 EDTA solution, and to a lesser extent in the pH 7.0 EDTA solution, it seems that the pseudo-steady state thickness of the passive layer is not affected by EDTA. Assuming that the passive layer behaves as a dielectric then the measured capacitance, at high frequencies, will

be proportional to the thickness of the layer. Indeed, Van der Linden et al. [16] have shown that the capacitance calculated from the impedance is directly proportional to the oxide layer thickness on aluminium. It can be seen from Figure 3 that essentially identical capacitance–voltage curves are recorded in the presence and absence of EDTA at a given pH. There is a large frequency dispersion in the capacitance, as can be seen for the plots recorded at 1 and 5 kHz for the pH 7.0 solution, but this is consistent with the amorphous nature of such oxide layers and has been reported previously for many systems [17, 18]. To maintain a constant film thickness it seems that the EDTA ligands attack both the outer layers of the oxide film and consume some of the Al^{3+} species, which are transported to the oxide–solution interface during further oxide formation. This process, with the destruction of the outer aluminium hydroxy species, or aluminium hydroxy chloride species which are formed in chloride environments [19], will lead to a modification of the properties of the oxide–solution interface.

It is interesting also that although enhanced dissolution of the oxide layer occurs that the EDTA does not have any significant deleterious effect on pit initiation. This is evident from the data presented in Figure 11, where the cumulative probability distribution curves for pit initiation in the presence and absence of EDTA in a molybdate-containing solution are essentially identical. In fact, EDTA inhibits pit initiation in the non-molybdate solution. This is due to an EDTA-induced buffering action, an action which inhibits the formation of the acidic pit solution. Because the EDTA attacks the outer hydroxy layers it should also alter the adsorption characteristics of the oxide. This, combined with the fact that the presence of EDTA in the molybdate-containing solution has little effect on the pitting potential, points strongly to the rate-determining step for pit initiation, in this case, being the establishment of a critical pit solution [7, 8].

The impedance data recorded in the absence of EDTA are consistent with a simple Randles circuit where R_1 represents the charge-transfer resistance. These data are time-dependant during the early stages of polarization, but reach a steady-state condition after about 90 min. There is little difference in the charge-transfer resistance, or the impedance for the pH 7.0 and 9.0 solutions. However, the data are very different, characterised by a capacitive region at high frequencies, an inductive region at intermediate frequencies and a second capacitive region at low frequencies, indicative of a much more complex system in the presence of EDTA. Such inductive behaviour, as seen in the intermediate frequency regions, indicates that the increasing oxidation current is impeded by an inductive current flowing in the opposite direction. This inductive current has previously been ascribed to localized corrosion of aluminium in chloride solutions [20, 21], and to the adsorption of intermediates [22]. There was no evidence of any pitting attack on the aluminium electrodes at the potentials chosen for the impedance measurements in this study. This tends to suggest that the inductive impedance arises from the adsorption of intermediate species generated by the intense EDTA-induced dissolution of aluminium. These intermediate species may be transient $Al(EDTA)^{3-}$ or the complexation product, $Al(EDTA)^{-}$. The low frequency capacitive response may also be related to these adsorbed species. The large values of the capacitance in this low frequency region, of the order of 3 mF cm^{-2}, suggests that the adsorbed species form a large capacitive network. As in the d.c. experiments these effects are more intensified in the pH 9.0 electrolyte where EDTA complexation with aluminium is more thermodynamically favoured.

5. Conclusion

A significant increase in the rate of anodic dissolution of aluminium was observed in alkaline solutions on the introduction of EDTA into the solution. The presence of EDTA in solutions of pH 4.0 or less had no observable activating effect on aluminium. These findings are consistent with the relative stabilities of the $Al(EDTA)^{-}$ complex which are more thermodynamically favoured under alkaline conditions. EDTA had a slight inhibiting action on pitting attack in the alkaline solutions. This was associated with the buffering action of EDTA, which inhibited the formation of a critical pit solution. But, in the presence of molybdate anions EDTA had no influence on the pitting process. The impedance spectra recorded in the alkaline EDTA solutions are consistent with the adsorption of EDTA complex species at the surface, which, at low frequencies, exhibit large capacitance values.

Acknowledgements

The authors gratefully acknowledge the support of this work by Enterprise Ireland, under the Basic Science Research Grants Award (projects code SC/96/456).

References

1. D.C. Harris, 'Quantitative Chemical Analysis', 2nd edn (Freeman & Co., New York, 1987), p. 272.
2. J.W. Palmer and P.J. Boden, *Br. Corrosion J.* **27** (1002) 305.
3. A. Nahle, *Bull. Electrochem.* **14** (1998) 52.
4. K.E. Healy and P. Ducheyne, *J. Materials Sci.* **4** (1993) 117.
5. J.N. Alhajji and M.R. Reda, *J. Electrochem. Soc.* **141** (1994) 1432.
6. G. Capobiance, C. Goatin, G. Moretti, S. Patron and L. Toniolo, *Corrosion* **50** (1994) 886.
6. J.R. Galvele, *J. Electrochem. Soc.* **12** (1976) 464.
7. J.R. Galvele, *Corros. Sci.* **21** (1981) 551.
8. G.M. Treacy, PhD thesis, National University of Ireland (1997).
9. W.M. Carroll and C.B. Breslin, *Corros. Sci.* **33** (1992) 1161.
10. C.B. Breslin and W.M. Carroll, *Corros. Sci.* **34** (1993) 317.
11. J.R. Macdonald, 'Impedance Spectroscopy' (J. Wiley & Sons, New York, 1987).

12. D.R. Franceschetti and J.R. Macdonald, *J. Electroanal. Chem.* **82** (1977) 271.
13. D. Armstrong, *J. Electroanal. Chem.* **34** (1972) 387.
14. R.F.A. Jargelius-Pettersson and B.G. Pound, *J. Electrochem. Soc.* **145** (1998) 1462.
15. B. Van der Linden, H. Terryn and J. Vereecken, *J. Appl. Electrochem.* **20** (1990) 798.
16. A Di Paola, D. Shukla and U. Stimming, *Electrochim. Acta.* **36** (1991) 345.
17. G. Tuccio, S. Piazza, C. Sunseri and F. Di. Quarto, *J. Electrochem. Soc.* **146** (1999) 493.
18. R.T. Foley and T.H. Nguyen, *J. Electrochem. Soc.* **129** (1982) 464.
19. J.B. Bessone, D.R. Salinas, C.E. Mayer, M. Ebert and W.J. Lorenz, *Electrochim. Acta.* **37** (1992) 2283.
20. L. Chen, N. Myung, P.T.A. Sumodjo and K. Nobe, *Electrochim. Acta.* **44** (1999) 2751.
21. M. Cai and S.M. Park, *J. Electrochem. Soc.* **143** (1996) 3895.